Fifth-order intensity autocorrelations based on six-wave mixing of femtosecond laser pulses

Eugenijus Gaižauskas,* Kęstutis Steponkevičius, and Virgilijus Vaičaitis
Laser Research Center, Vilnius University, Saulėtekio 10, Vilnius LT-10223, Lithuania
(Received 28 October 2015; published 8 February 2016)

It is shown both experimentally and by numerical simulations that fifth-order intensity autocorrelations of femtosecond laser pulses can be obtained from two-beam noncollinear six-wave mixing in air. A numerical analysis of competing direct and six-wave-assisted third-harmonic-generation pathways showed that these measurements are suitable for the background-free temporal characterization of laser pulses. Reshaping of the pulse and 10 fs subpulse formation during the primary stages of light filamentation were observed using the proposed method.

DOI: 10.1103/PhysRevA.93.023813

I. INTRODUCTION

While the spectrum and energy of laser pulses can be relatively easily and reliably registered using standard laboratory equipment, this is not the case when the temporal parameters of laser pulses have to be measured. The simplest approach, which has been used for a long time to estimate laser pulse duration and other temporal characteristics, is that of second-order intensity autocorrelation measurements [1,2]. Though this method allows a credible estimation of the pulse duration, the second-order autocorrelation trace is always symmetric, regardless of the test-pulse symmetry, i.e., it cannot resolve the time ambiguity [2]. In addition, second harmonic autocorrelation measurements require broadband phase matching, which in the case of ultrashort pulses requires very thin nonlinear crystals [3]. On the other hand, sophisticated pulse characterization methods, such as frequency-resolved optical gating (FROG) [4] and spectral phase interferometry for direct electric field reconstruction (SPIDER) [5], are now widely available commercially and used in laboratories to precisely measure the electric field characteristics of an optical pulse. However, these methods are quite complex and simple autocorrelation-based pulse-duration measurements are still in use.

It should be stressed in this context that the characterization of laser pulses scales well with the autocorrelation order, and, importantly, higher-order autocorrelations (apart from the pulse duration) may provide additional information about pulse asymmetry and substructure. Therefore, in this report, we propose a favorable option for fifth-order correlation measurements based on two-beam noncollinear six-wave mixing (SWM) in air, which allows temporal characterization of powerful femtosecond laser pulses.

In order to demonstrate the advantages of higher-order autocorrelations, the plots of a bimodal (having two bell-shaped Gaussian intensity humps) test function together with its second-order (left panel) and fifth-order (right panel) autocorrelation functions, defined as $G^{(n)}(\tau) = \int_{-\infty}^{\infty} I_L^{n-1}(t) I_L(t-\tau)dt$, with $n = 2$ and $n = 5$, are plotted in Fig. 1. It is easy to notice that the fifth-order autocorrelation trace indeed shows the realistic temporal intensity of the pulse. (Note that straightforward evaluation shows that the width of the nth-order autocorrelation traces scales as $\sqrt{n/(n-1)}\tau_L$ compared with the width of the Gaussian pulse τ_L). Therefore, the main drawbacks of pulse characterization by second-order autocorrelations can be overcome by measuring the higher-order autocorrelations. Moreover, apart from nonlinear crystals, these measurements can be performed in solid isotropic materials, liquids, and even gaseous media, which usually have a much higher optical damage threshold and can recover from the damage.

II. NONCOLLINEAR SIX-WAVE MIXING IN AIR

Recently, it has been demonstrated that two-beam noncollinear SWM provides strong signal generation at the third harmonic frequency in air within a wide range of input laser powers [6,7]. The third harmonic observed appears to be due to noncollinear six-wave phase matching in normally dispersive media, and its high directionality allows registration of background-free autocorrelations at high-input pulse intensities. In contrast, strict phase-matching conditions for direct third harmonic generation (THG), which is usually used for measuring third-order autocorrelations, cannot be satisfied in normally dispersive isotropic media [8]. Therefore, direct THG is possible only in the narrow spectral regions of anomalous dispersion in resonant gases [9].

Further, we consider the specific case of THG in two-beam pump geometry (shown in Fig. 2) that separates out the phase-matched background-free third harmonic signal fields with complex amplitudes $\mathcal{E}_{\mathrm{TH}}^{(1,2)}$ obtained through the SWM and direct THG signal (if any) in an instantaneous two-dimensional mapping.

Thus, in the absence of resonances, the SWM process can be interpreted as

$$\mathcal{E}_{\mathrm{TH}} = \mathcal{E}_{\mathrm{TH}}^{(1)} + \mathcal{E}_{\mathrm{TH}}^{(2)} \sim \chi^{(5)}\left(\mathcal{E}_L^{(1)4}\mathcal{E}_L^{(2)*} + \mathcal{E}_L^{(2)4}\mathcal{E}_L^{(1)*}\right), \qquad (1)$$

where $\mathcal{E}_L^{(1,2)}$ denotes the complex amplitudes of the fundamental field in different pump beams, and $\chi^{(5)}$ is the nonresonant fifth-order nonlinear susceptibility. In our SWM geometry, light-matter interaction at the fundamental frequency ω produces a third harmonic signal at frequency $\omega_{\mathrm{TH}} = 4\omega^{(1,2)} - \omega^{(2,1)}$, where the superscripts 1 and 2 indicate that the fields from different pump beams are involved. Since during our experiments the signal energy at the third harmonic frequency is measured in one of the generation channels,

*eugenijus.gaizauskas@ff.vu.lt

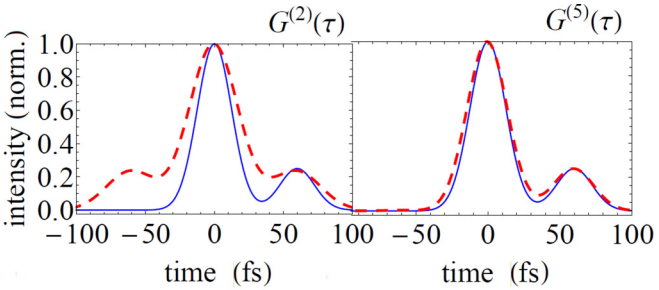

FIG. 1. Plots of a bimodal test function (solid blue lines) and corresponding second- and fifth-order intensity autocorrelation functions (red dashed lines) on the left and right panels, respectively.

a variation in the time delay τ between two pump pulses gives a signal $\sim|\mathcal{E}_{\mathrm{TH}}^{(1)}|^2$ in the form of a fifth-order intensity autocorrelation function $G^{(5)}(\tau)$ of the fundamental pulse.

It should be remembered that in the wave-mixing process, a phase-matching bandwidth is defined by the function $\mathrm{sinc}^2(\Delta kL/2)$, where Δk is the phase mismatch between the frequencies of the fundamental and third harmonic pulses, and L stands for the interaction length. Note that due to the low air dispersion and small interaction angles necessary for efficient SWM, extremely broad phase-matching bandwidths can be obtained (see Fig. 3), which under typical experimental conditions (central laser wavelength of 800 nm) are more than 60 nm and support pulse duration measurements as short as 5 fs.

In comparison to direct THG, SWM is a higher-order process and usually is expected to be much less efficient than the former. However, under our experimental conditions, the SWM is perfectly phase matched ($\Delta k = 0$ at 800 nm), which is not the case for direct THG. In addition, we notice that the ratio r_{nl} of nonlinear lengths for four-wave mixing (FWM) and SWM scales with the intensity of the fundamental wave:

$$r_{\mathrm{nl}} = L_{\mathrm{nl}}^{\mathrm{FWM}}/L_{\mathrm{nl}}^{\mathrm{SWM}} = \frac{n_4}{n_2}|\mathcal{E}_L|^2. \tag{2}$$

Here, n_2,n_4 are the nonlinear indexes of refraction for the FWM and SWM processes, respectively. Taking $n_2 = 3\times 10^{-10}$ cm^2/GW and $n_4 = 10^{-14}$ cm^4/GW^2 [10], the ratio given by Eq. (2) approximates to unity for $\mathcal{E}_L^2 = 30$ TW/cm^2, whereas for the conditions close to our experiment ($\tau_L = 35$ fs, pulse energy 0.6 mJ, and beam waist 100 μm), the intensity of the fundamental wave $\mathcal{E}_L^2 \simeq 200$ TW/cm^2. Thus, under our experimental conditions, the ratio $r_{\mathrm{nl}} \simeq 7$, which clearly indicates that the SWM signal is much stronger than that of the direct THG.

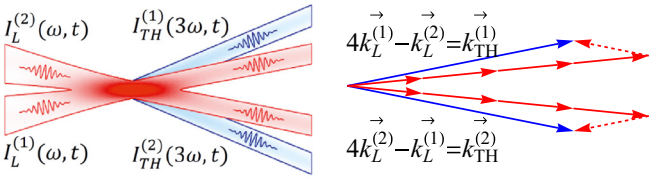

FIG. 2. Left: Configuration of the pump $I_L(t)$ and THG $I_{\mathrm{THG}}(t)$ beams during phase-matched noncollinear SWM in air. Right: A wave-vector diagram of the same process.

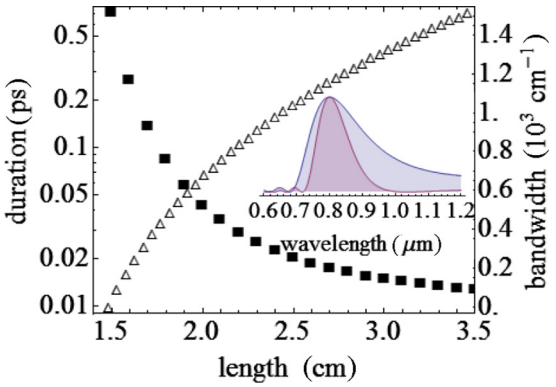

FIG. 3. Calculated phase-matching bandwidths (black squares, right axis) for SWM in air and evaluated durations for the corresponding bandwidth-limited pulses, plotted on a logarithmic scale vs the interaction length L. The inset shows phase-matching bandwidth shapes for $L = 3.5$ and 2 cm.

In order to reveal in more detail the competition between two pathways (direct THG and THG assisted by SWM), we have performed some simplified numerical experiments estimating the conversion efficiency of both processes. Specifically, we performed simulations considering paraxial propagation along the z axis of linearly polarized laser beams having wave numbers k_L and k_{th}, as well as wavelengths of 800 and 267 nm, respectively. For the sake of simplicity, the cylindrical symmetry of the complex scalar envelopes for all three beams was assumed and the effects related to the pulse group velocity and dispersion were neglected. Comparison of the efficiency of direct THG and noncollinear THG assisted by SWM (described above) was performed including self-focusing and nonlinear losses due to multiphoton absorption in the modified nonlinear Schrödinger (NLS) equation in $2+1$ dimensions, and also disregarding depletion of the pump beam. In the frame of the adopted paraxial approximation, the resulting equation for the pump amplitude $\mathcal{E}_L(r,z,t)$ then reads

$$\frac{\partial\mathcal{E}_L}{\partial z} = \left(\frac{i}{2k_L}\Delta_r + ik_Ln_2|\mathcal{E}_L|^2 - \frac{\beta^{(K)}}{2}|\mathcal{E}_L|^{2K-2}\right)\mathcal{E}_L, \tag{3}$$

where r and Δ_r stand for the radial coordinate and Laplace operator, respectively, z is the distance of propagation, $\beta^{(8)} = 4\times 10^{-98}$ cm^{13} W^{-7} is a multiphoton absorption (MPA) coefficient, and $n_2|\mathcal{E}_L|^2$ stands for the intensity-dependent changes in the refraction index.

Assuming that the optical nonlinearities of the medium are induced by the pump beam, and if we disregard MPA and the nonlinear self-action of the weak generated fields, then the equations for the slowly varying complex amplitudes of third harmonic fields in the retarded coordinate system read as follows:

$$\frac{\partial\mathcal{E}_d}{\partial z} = \frac{i}{2k_{\mathrm{th}}}\Delta_r\mathcal{E}_d + ik_{\mathrm{th}}\left(n_2|\mathcal{E}_L|^2\mathcal{E}_d + n_4\mathcal{E}_L^3\right), \tag{4}$$

$$\frac{\partial\mathcal{E}_s}{\partial z} = \frac{i}{2k_{\mathrm{th}}}\Delta_r\mathcal{E}_s + ik_{\mathrm{th}}\left(n_2|\mathcal{E}_L|^2\mathcal{E}_s + n_4\mathcal{E}_L^4\mathcal{E}_L^*\right), \tag{5}$$

where $\mathcal{E}_d$ and $\mathcal{E}_s$ are third harmonic amplitudes rising from both the direct and SWM-assisted THG processes, respectively

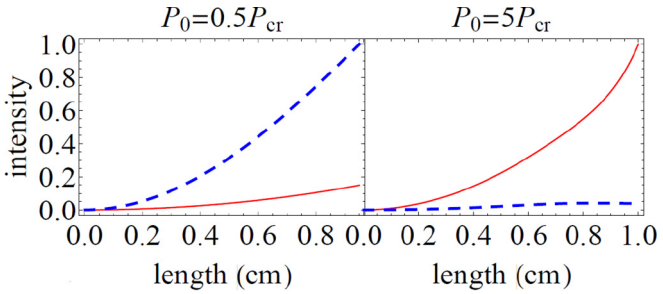

FIG. 4. Numerically evaluated, according to Eqs. (2)–(4), generation efficiencies for the direct (blue dashed line) and SWM-assisted (red line) THG pathways. The results are normalized to maximal value at $z = 1$ cm and plotted for $P_0 = 0.5P_{cr}$ and $P_0 = 5P_{cr}$ on the left and right panels, respectively.

(group velocities of all three pulses were assumed to be equal). Both signals were evaluated at the distance $L = 1$ cm for the incident beam power $P_0 = E_0/\tau_L\sqrt{\pi/2}$ (at the Gaussian pulse maximum), where E_0 is the pulse energy at the input. Accordingly, the initial pump amplitude can be expressed as $\mathcal{E}_L^0 = \sqrt{2P_0/\pi w_0^2}$, where w_0 stands for the beam waist.

The results of the numerical calculations are presented in Fig. 4. It can be seen that while at relatively low pump power direct THG prevails over noncollinear (resulting from SWM), the latter dominates under intensities that appear close to those used in our experiments. Specifically, taking pump power of $5P_{cr}$, for the critical power for self-focusing in air $P_{cr} = 3$ GW, laser pulse energy appears to be 0.5 mJ for a 35 fs pulse duration. In this case, the ratio of SWM-assisted and direct THG signals exceeds 20 for the interaction length of 1 cm, which was the case during our experiment. Moreover, since these two third harmonic beams can be well separated spatially, one may expect the SWM signal (and, accordingly, the fifth-order autocorrelation) to be registered within a wide range of pump power and with a high signal-to-noise ratio.

III. EXPERIMENT

The experimental setup was similar to that used in our previous studies (see Fig. 1 in [7] for the details). The pulse energy of the femtosecond Ti:sapphire laser (central wavelength 800 nm, maximal pulse energy 8.0 mJ) could be varied by an attenuator composed of a zero-order half-wave plate and a broadband polarizer. The laser beam was divided with a 50:50 beam splitter and the resulting two beams were focused in ambient air by a lens of 100 cm focal length. The polarization state of the beams was controlled by an additional half-wave plate inserted in the path of one of the beams. The laser beams were crossed at a small angle in the focal plane of the focusing lens, where a strong third harmonic signal in the directions defined by the phase-matching conditions (see Fig. 2) was generated [6,7]. The third harmonic and fundamental laser beams were therefore well separated spatially. However, in order to improve the signal-to-noise ratio for the third harmonic energy measurements, we also used additional dichroic mirrors and calibrated optical filters. It should be noted that although the most efficient THG was observed at a pump beam crossing angle of about 13 mrad, when phase-matching conditions of noncollinear SWM were satisfied, two third harmonic beams could be observed over a wide range of beam crossing angles.

It should also be noted that during the experiment, laser pulse energy was kept below the level of SWM signal saturation due to laser-induced plasma formation and other competing nonlinear effects. Thus, for laser pulses of 35 fs (FWHM) duration, the generated SWM signal started to saturate when the total laser pulse energy exceeded 1.5 mJ.

An optical delay line inserted into the path of one of the beams allowed us to vary the time delay τ between the two pump pulses and to register their fifth-order autocorrelation. In addition, in order to monitor the duration of laser pulses, we also used a noncollinear second harmonic (SH) autocorrelator. The SH autocorrelations were recorded by placing a thin beta barium borate (BBO) crystal in the beam crossing region and varying the time delay τ between the pulses. However, in order to avoid optical damage of the crystal, laser pulse energies were significantly reduced during these measurements.

The width of the second-order autocorrelation was found to be 49.5 fs (FWHM), which corresponds to the actual laser pulse width of 35 fs (assuming the Gaussian pulse shape) or 32 fs (assuming the hyperbolic secant-squared pulse shape). As was expected, the width of fifth-order autocorrelations was much smaller: for the parallel pump beam polarizations, it was estimated to be 38.4 fs, while for the perpendicular pump polarizations, it was almost equal to 39 fs. According to the scaling presented above for the nth-order autocorrelation widths, this corresponds to 34.35 and 34.88 fs, respectively. As the use of parallel pump polarizations has led to slightly underestimated pulse-duration values, we discuss further only the case of orthogonal pump beam polarizations. Note that this tendency (shortening of autocorrelation width in the case of parallel laser-beam polarizations) was even more pronounced when using longer laser pulses (of the order of 100 fs), which can be explained by taking into account the pulse transformation during parametric interactions, demonstrated for three- and four-wave mixing [11,12].

IV. RESULTS AND DISCUSSION

Logarithmic plots of the experimentally recorded $G^{(5)}(\tau)$ traces are presented in Fig. 5 (black squares) for laser pulses of 35 fs duration. It can be seen that for the total pump pulse

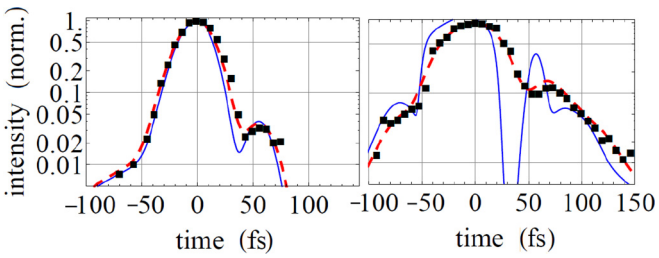

FIG. 5. Black squares: logarithmic plots of experimentally measured (using SWM in air) fifth-order autocorrelations from 0.6 mJ (left panel) and 0.8 mJ (right panel) pump pulses with 35 fs durations at FWHM. The blue solid line marks the recovered intensity of the pulse obtained by fitting its fifth-order correlation function (red dashed line) to the experimental data.

energy of 0.6 mJ, the autocorrelation trace (left panel) remains practically symmetric above level 10^{-1} from the maximum of the pulse amplitude. However, the second satellite spike at the 10^{-2} level in the trailing part can easily be seen, which indicates that under given experimental conditions the early stages of beam filamentation are already taking place. This assumption is confirmed further by studying the experimentally recorded autocorrelation traces for the 0.8 mJ total pump pulse energy (Fig. 5, right panel). In this case, one can observe flattening of the main peak as well as splitting (formation of subpulses in the trailing and leading parts) of the laser pulse, characteristic of propagation beyond the nonlinear focus during femtosecond filamentation [13]. A subpulse with a duration as short as 10 fs in the trailing part of the pulse (blue solid line) was observed by fitting its fifth-order correlation function (red dashed line) to experimental data, and this fact further supports our prediction that SWM is capable of characterizing extremely short pulses.

However, since the SWM is efficient only when pump pulses are of high intensity, their propagation to the interaction region may become highly nonlinear, which results in their temporal reshaping. Such pulse reshaping took place even at the lowest pump pulse energies (see Fig. 5). In order to avoid or reduce this effect, one should make the path of free propagation in nonlinear media as short as possible.

In the case of extremely short laser pulses, the geometrical constraints should also be taken into account because pulse fronts in the crossed beams also are not parallel, which prolongs their interaction time. Thus, given that the beam crossing angle is 10 mrad, the 100-μm-wide beam (which was the case in our experiment) widens the width of the correlation function by about 3 fs. Therefore, the wider the laser beams are, the bigger the measurement error, which limits the minimum pulse duration that can be measured. On the other hand, in the case of wide laser beams and short test pulses, single-shot measurements when the delay time is related to the spatial beam coordinate [14] are, in principle, possible. In addition, a slight modification of our experimental setup (simultaneous registration of signal spectra) may allow for SWM-modified frequency-resolved optical gating measurements (SWM-FROG), which are expected to provide better resolution than that obtained by using conventional autocorrelations [15].

V. CONCLUSIONS

In conclusion, we have shown that fifth-order autocorrelation functions of femtosecond laser pulses can be obtained using two-beam noncollinear SWM in air, which allows simple and reliable temporal characterization of short laser pulses. The advantages of the proposed fifth-order autocorrelations are the simplicity of their recording, their validity in a wide range of wavelengths, and their ability to reveal the asymmetry of femtosecond laser pulses. Taking advantage of the low dispersion and high optical damage threshold in air, this approach can be used for the characterization of laser pulses as short as 5 fs. Finally, using the proposed method, it is possible to investigate light propagation processes that result from extremely high light intensities (e.g., femtosecond filamentation in transparent media) when no physical objects can be placed in the path of the laser beams.

[1] D. J. Bradley and G. H. C. New, Proc. IEEE **62**, 313 (1974).
[2] I. A. Walmsley and C. Dorrer, Adv. Opt. Photon. **1**, 308 (2009).
[3] M. Nisoli, S. D. Silvestri, O. Svelto, R. Szipöcs, K. Ferencz, C. Spielmann, S. Sartania, and F. Krausz, Opt. Lett. **22**, 522 (1997).
[4] R. Trebino, *Frequency-Resolved Optical Gating: The Measurement of Ultrashort Laser Pulses* (Kluwer Academic, Boston, 2002).
[5] C. Iaconis and I. A. Walmsley, IEEE J. Quantum Electron. **35**, 501 (1999).
[6] V. Vaičaitis, V. Jarutis, K. Steponkevičius, and A. Stabinis, Phys. Rev. A **87**, 063825 (2013).
[7] K. Steponkevičius, B. Makauskas, E. Žeimys, V. Jarutis, and V. Vaičaitis, Laser Phys. Lett. **12**, 025402 (2015).
[8] R. W. Boyd, *Nonlinear Optics*, 2nd ed. (Academic, San Diego, 2003).
[9] G. G. Grigoryan, A. O. Melikyan, D. G. Sarkisyan, and A. S. Sarkisyan, Quantum Electron. **25**, 262 (1995).
[10] V. Loriot, E. Hertz, O. Faucher, and B. Lavorel, Opt. Express **17**, 13429 (2009); **18**, 3011 (2010).
[11] E. Gaizauskas, R. Grigonis, and V. Sirutkaitis, J. Opt. Soc. Am. B **19**, 2957 (2002).
[12] Y. Li, L. Qian, D. Lu and D. Fan, J. Opt. A: Pure Appl. Opt. **8**, 689 (2006).
[13] A. Couairon and A. Mysyrowicz, Phys. Rep. **441**, 47 (2007).
[14] F. Salin, P. Georges, G. Roger, and A. Brun, Appl. Opt. **26**, 4528 (1987).
[15] Y. Nomura, H. Shirai, and T. Fuji, Nat. Commun. **4**, 2820 (2013).